Improvement of interfacial friction factor for the prediction of void fraction in the nearly horizontal flow

Tae-Hwan Ahn, Jae-Jun Jeong, Byong-Jo Yun*
Department of Mechanical Engineering, Pusan national university,
Busandaehak-ro, 63 beon-gil, Geumjeong-gu, Busan, 609-735, Korea
**Corresponding author: bjyun@pusan.ac.kr*

1. Introduction

The Korean advanced nuclear power plant APR+ is expected to adopt a passive auxiliary feedwater system (PAFS) consisting of a condensation heat exchanger having nearly horizontal tubes (3° downward) as one of the passive safety systems. Recently, many experimental studies and analyses have been revealed that the most of existing empirical type correlations underestimate the heat transfer coefficient in the horizontal tubes of condensing heat exchanger similar to that of PAFS [1]-[3]. As an alternative approach to achieve better prediction, a mechanistic condensation model is considered applicable to the nearly horizontal tubes by treating two different heat transfer mechanisms in the separated flow regimes typically observed in the PAFS heat exchanger tubes [4]. For such approach, an estimation of void fraction is of importance to consider different heat transfer mechanisms in the nearly horizontal condensing tubes. Therefore, the objective of this study was to develop a new mechanistic model for the prediction of void fraction in the separated flows in a nearly horizontal tube, especially focusing on continuous changes of the geometric shape and friction factor for the phase interface. That is, geometric relations that assumed an ideal arc for the curved interface were used to define the flow regime transition from stratified flow to annular flow continuously. Furthermore, the interfacial friction factor was also studied for each flow regime by using experimental data available in the open literatures.

2. Void fraction prediction model

2.1 Two-fluid momentum balance

The proposed model is based on the concept of equilibrium separated flow firstly proposed by Taitel and Dukler [5]. The configuration of the ideal separated flow, which is typically generated in the nearly horizontal tube, is schematically depicted in Fig. 1.

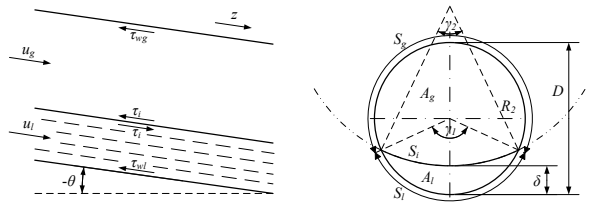

(a) flow parameters (b) geometric parameters

Fig. 1. Schematic descriptions of the separated flow configuration

The one–dimensional momentum balance equation for two phases is given as follows in the fully developed steady state flow:

$$\frac{\tau_{wg}S_g}{A\alpha}-\frac{\tau_{wl}S_l}{A(1-\alpha)}+\frac{\tau_i S_i}{A\alpha(1-\alpha)}-(\rho_l-\rho_g)g\sin\theta=0 \quad (1)$$

To determine the void fraction by using Eq. (1), it is necessary to define the constitutive equations for the shear stresses τ_{wg}, τ_{wl} at the wall and τ_i at the phase interface, as well as for the contact perimeters S_g, S_l, and S_i over which the shear stresses act.

The shear stress terms for the wall and interface are calculated by applying single-phase expressions as follows,

$$\tau_{wg}=\frac{1}{2}f_g\rho_g u_g{}^2; \qquad \tau_{wl}=\frac{1}{2}f_l\rho_l u_l{}^2 \quad (2)$$

$$\tau_i=\frac{1}{2}f_i\rho_g|u_g-u_l|(u_g-u_l) \quad (3)$$

where the actual velocities u_g and u_l are expressed by the superficial velocities j_g and j_l, respectively, as well as function of the mass flux G, flow quality x, and void fraction α as shown below,

$$u_g=\frac{j_g}{\alpha}=\frac{Gx}{\rho_g\alpha};\ u_l=\frac{j_l}{(1-\alpha)}=\frac{G(1-x)}{\rho_l(1-\alpha)} \quad (4)$$

Additionally, the friction factors f_g and f_l are obtained by the Blasius' correlation as follows,

$$f_g=\frac{c_g}{(\rho_g u_g D_{hg}/\mu_g)^{n_g}}; \qquad f_l=\frac{c_l}{(\rho_l u_l D_{hl}/\mu_l)^{n_l}} \quad (5)$$

where μ_g and μ_l are the dynamic viscosities of the gas and liquid phases, respectively, and the hydraulic equivalent diameters in the corresponding phases are given by

$$D_{hg}=\frac{4A_g}{S_g+S_i}; \qquad D_{hl}=\frac{4A_l}{S_l} \quad (6)$$

For both friction factors, the constants c and n were defined as 16 and 1.0, respectively, for laminar flow; the corresponding values for turbulent flow were set to 0.046 and 0.2.

The phase interface appeared in Fig. 1b is assumed to be an ideal arc shape which changes continuously according to flow conditions. The geometric relations of the flow cross-section are defined by trigonometric relationships under the condition of downward concave curvature ($\gamma_1>\gamma_2$). From the relationships, the void fraction and contact perimeters are obtained as follows.

$$\alpha = 1 - \frac{\gamma_1 - \sin\gamma_1}{2\pi} + \frac{\gamma_2 - \sin\gamma_2}{2\pi}\left(\frac{1-\cos\gamma_1}{1-\cos\gamma_2}\right) \quad (7)$$

$$S_g = \pi D - \gamma_1 (D/2); \qquad S_l = \gamma_1 (D/2) \quad (8)$$

$$S_i = \frac{\gamma_2 D \sin(\gamma_1/2)}{2\sin(\gamma_2/2)}. \quad (9)$$

2.2 Flow regime transition model

To calculate the void fraction, flow regimes must be identified because they affect the geometric parameters expressed in Eqs. (7)-(9), and the interfacial friction factor in Eq. (3). The separated flow regimes expected in the horizontal heat exchanger tubes are typically classified into stratified-smooth flow, stratified-wavy flow, and annular flow. Fig. 2 continuously depicts the ideal interfacial shapes for such flow regimes. The stratified-smooth flow, whose interface is basically flat, occurs under the low superficial velocities for gas and liquid phases. As the gas superficial velocity increases at a given liquid flow condition, the flow regime developed to stratified-wavy flow in which liquid tends to climb up the tube wall and then the curvature of the interface becomes far away from flat owing to an enhanced interfacial shear stress [6]. As the superficial gas velocity increases further, the liquid film eventually occupies the entire wall of the tube which is identified as an annular flow regime.

From these geometrical models, the conditions for flow regime transition among the stratified-smooth, the stratified-wavy flow and the annular flow were derived by the change of the interfacial shape which was assumed to be an ideal arc. The transition between stratified-smooth and stratified-wavy flows is assumed to occur when the wetted angle γ_1 in Fig. 2 is equal to the stratification angle γ_{ss} defined under the flat interfacial configuration. In contrast, the transition between stratified-wavy flow and annular flow was defined as the condition in which the wetted angle becomes 2π. In general, the region classified as the annular flow also includes the intermittent and dispersed flow regimes under high liquid flow conditions. Such flow regimes occur when the void fraction calculated in the annular configuration is less than 0.76 which is spontaneous blockage criterion proposed by Barnea [7]. Thome et al. [8] considered the intermittent and dispersed flow regimes as annular flow in their condensation heat transfer model. However, the intermittent and dispersed flow regimes were not considered in the present study because our study is limited to the separate flows.

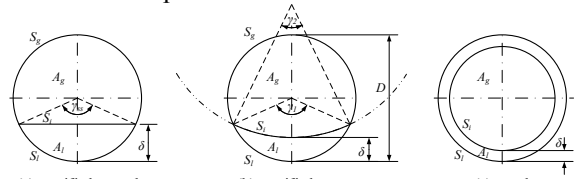

Fig. 2. Ideal interfacial shapes for separated flow regimes in the horizontal tube

2.3 Constitutive relations according to the flow regimes

2.3.1 Geometrical parameters

Geometrical relation for the stratified-smooth flow regime is basically obtained by Taitel and Dukler [5] based on flat interface. In the present model stratified-smooth flow represented by a flat interface occurs when the central angle γ_2 of the eccentric arc is set to be zero (see Fig. 2a). Substituting the condition into Eq. (7), the wetted angle for the flat interface is implicitly calculated from following equation.

$$\alpha = 1 - \frac{\gamma_1 - \sin\gamma_1}{2\pi}. \quad (10)$$

According to Eq. (9) when $\gamma_2 \to 0$, the interfacial contact perimeter is defined as

$$S_i = D\sin(\gamma_1/2). \quad (11)$$

Stratified-wavy flow was assumed to have concave downward interface shape of an ideal arc. Fig. 2b shows the geometrical configuration for this flow regime and the relevant geometric parameters were defined in Eqs. (7)-(9). The wetted angle which is requisite parameter for the calculation of wall contact perimeter and also void fraction is calculated from following correlation proposed by Hart et al. [9].

$$\gamma_1 = 2\pi\left(0.52(1-\alpha)^{0.374} + 0.26Fr^{0.58}\right) \quad (12)$$

$$Fr = \frac{\rho_l u_l^{\,2}}{(\rho_l - \rho_g) Dg\cos\theta} \quad (13)$$

An inclination angle θ added in the Froude number Fr is to take into account the orientation of the flow channel, differing from the original form used by Hart et al. for the horizontal flow.

Annular flow is a limiting condition for both wetted angle γ_1 and the central angle γ_2 of which values are 2π (see Fig. 2c). Assuming symmetric shapes of interface in the annular flow, the void fraction is simply expressed as the function of annular film thickness as follow,

$$\alpha = \left(1 - \frac{2\delta}{D}\right)^2. \quad (14)$$

Similarly, the interface perimeter can be expressed by

$$S_i = \pi(D - 2\delta). \quad (15)$$

For the annular flow, the void fraction calculated by the constitutive models above needs to be satisfied the value of more than 0.76 by spontaneous blockage criterion [7].

2.3.2 Interfacial friction factor

The interfacial friction factor appeared in the Eq. (3) has a significant effect on the calculation of void fraction by momentum balance equation as in Eq. (1) and is changeable according to the flow regimes. In the present study, the interfacial friction factors fi were

widely investigated across the flow regime using the present model with experimental data for the separated flows in the horizontal and nearly horizontal pipes were collected from open literatures as in the Table. 1. The deduction results of the interfacial friction factor f_i from the data are expressed with gas phase wall friction factor f_g as shown in Fig. 3. The figure explicitly shows that the ratio of f_i to f_g is around unity for stratified-smooth, between 1 and 10 for stratified-wavy flow, and more than 10 for annular flow even though they have somewhat scattering to the experimental data.

From the results, the interfacial friction factor is assumed to be $f_i = f_g$ for the stratified-smooth flow and $f_i = 10f_g$ for the annular flow, founded on previous investigators [5, 17]. In contrast to these, f_i should be continuously changed from the stratified-smooth flow to the annular flow so as to ensure continuity in the void fraction predictions. In this study, f_i for the stratified-wavy flow is expressed by an angle γ^* normalized between flow regime transitions as follows,

$$\gamma^* = \frac{\gamma_1 - \gamma_{ss}}{2\pi - \gamma_{ss}} . \quad (16)$$

where γ_{ss} is the stratification angle for flat interface of the stratified-smooth flow.

By applying Eq. (16), the ratio of f_i to f_g is plotted with the normalized wetted angle under stratified-wavy flow as in the Fig. 4. Consequently, the interfacial friction factor correlation for the stratified-wavy flow is obtained by the regression analysis between stratified-smooth and annular flow boundaries as follows,

$$f_i = f_g(1 + 9\gamma^{*\,0.76}) . \quad (17)$$

Table I: Summary of experimental data for the interfacial friction factor and void fraction in the nearly horizontal pipes

Data of	Fluids	Inclination	I.D. (mm)	Pressure (bar)	Mass flux (kg/m^{2}s)	Flow quality	Void fraction	Flow regimes
France and Lahey [10]	Air-Water	Horizontal	19	1	7~1487	0~0.55	0.06~0.94	Stratified, Annular, Intermittent
Paras et al. [11]	Air-Water	Horizontal	50.8	1	32~139	0.10~0.65	0.89~0.99	Stratified,
Abdul-Majeed [12]	Air-Kerosene	Horizontal	50.8	1.97~ 8.43	2~1199	0.01~0.94	0.39~0.99	Stratified, Annular
Chen et al. [13]	Air-Kerosene	Horizontal	77.9	1	7~47	0.12~0.84	0.85~0.99	Stratified
Badie et al. [14]	Air-Water Air-Oil	Horizontal	78	1	18~79	0.29~0.97 0.37~0.97	0.89~0.99	Stratified
Ottens et al. [15]	Air-Water	1°, 2°down, Horizontal	52	1	10~29	0.29~0.81 0.36~0.78	0.91~0.99	Stratified
Srisomba et al. [16]	R-134a	Horizontal	8	6.27~ 7.70	664~ 1455	0~0.81	0.17~0.99	Stratified, Annular, Intermittent

Table II: Summary of error for the void fraction prediction by new model with experimental data

Data of	Stratified-smooth flow		Stratified-wavy flow		Annular flow		Average of all data	
	Number of data points	APD ABSPD (%)	Number of data points	APD ABSPD (%)	Number of data points	APD ABSPD (%)	Number of data points	APD ABSPD (%)
France and Lahey [10]	10	2.57 3.40	19	1.03 2.59	14	-2.26 2.45	43	-0.38 2.51
Paras et al. [11]	-	-	18	-0.19 1.06	1	0.47 0.47	19	-0.88 1.33
Abdul-Majeed [12] *	13	-6.54 11.10	23	-0.83 1.84	30	-3.82 3.82	66	-3.57 4.65
Chen et al. [13] *	9	-4.00 4.00	39	-1.88 1.88	-	-	48	-2.98 2.98
Badie et al. [14] *	20	-3.33 3.33	46	-0.21 1.13	-	-	66	-1.50 1.85
Ottens et al. [15] †	4	0.47 0.47	103	0.74 0.74	-	-	107	0.40 0.41
Srisomba et al. [16] *‡	-	-	-	-	51	-3.33 4.05	51	-3.33 4.05
Average of all data sets	-	-2.17 4.46	-	-0.22 1.54	-	-2.23 2.70		-1.31 2.46
Average of all data points	56	-2.86 5.05	248	-0.04 1.26	96	-3.29 3.71	400	-1.21 2.38
Average of all data points (Comparison with Taitel and Dukler [8] model)	63	-1.76 4.15	189	-1.10 1.43	148	-10.28 10.28	400	-4.60 5.13

*using non-water fluid
†including downward flow data
‡one-component two-phase flow

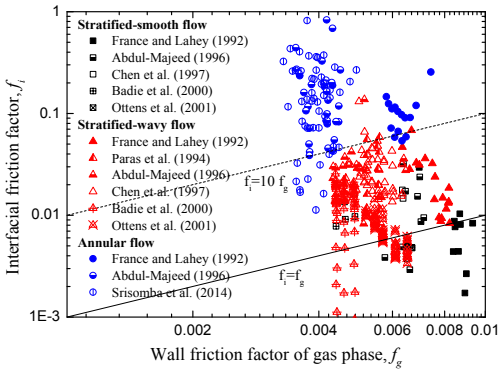

Fig. 3. Relationship between f_i and f_g in the separated flow

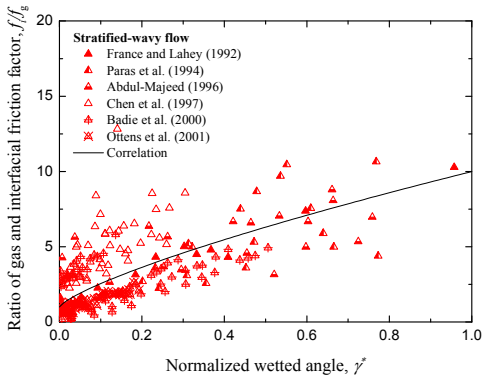

Fig. 4. Ratio of f_i to f_g with γ^* for the stratified-wavy flow

3. Calculations results and discussions

An iterative solution scheme for the void fraction is shown in Fig. 5. The experimental data in Table 1 were also used to evaluate the proposed void fraction prediction model. Among the data, France and Lahey's [10] data which measured the void fraction in the various flow regimes including stratified, annular, and intermittent flow was used for the evaluation of present proposed flow regime transition model. Fig. 6 shows that present model predicts the data fairly well, except for a few data points for intermittent flow that were incorrectly classified as stratified-smooth flow. The discrepancies are presumably caused by the uncertainty of the wetted angle correlation which plays an important role for the flow regime identification. Therefore, more reliable model for the wetted angle is requisite for the better prediction of flow regime.

The prediction capability is quantified by calculating the following two forms of deviations for each data point.

$$APD = \frac{\sum \alpha_{prd.} - \alpha_{exp.}}{\alpha_{exp.}} \times 100(\%) \quad (18)$$

$$ABSPD = \frac{\sum \left| \alpha_{pred.} - \alpha_{exp.} \right|}{\alpha_{exp.}} \times 100(\%) \ . \quad (19)$$

The former indicates whether the correlation over or under estimates the void fraction. The latter gives an indication of the average deviation regardless of its error direction.

Table 2 lists the APD and ABSPD for each data set and for the overall data according to flow regime. It shows that the prediction for the stratified-wavy flow is the most accurate with the APD of -0.04% and ABSPD of 1.26% for all data points. In contrast, the prediction for stratified-smooth flow has the highest ABSPD.

As compared in the Fig. 7, the present model shows better prediction capability compared with existing Taitel and Dukler model which has an especially larger discrepancy in annular flow data. The comparison results, as shown in Table 2, also indicate that the present model has improvements for the stratifies-wavy and annular flow compared with Taitel and Dukler model [5] because of improved interfacial shape and friction factor models. The proposed model, taken as a whole, predicts the void fraction with an APD of -1.21% and an ABSPD of 2.38% for all data points, which has better agreement than Taitel and Dukler model [5] showing an APD of -4.60% and an ABSPD of 5.13% for all data points.

The present model, however, generally tends to slightly under-predict the void friction showing negative values of the APD; the bias error appears to be particularly high for annular flow data as would be expected because the value of f_i used in the proposed model for annular flow is lower than that analyzed in Fig. 3.

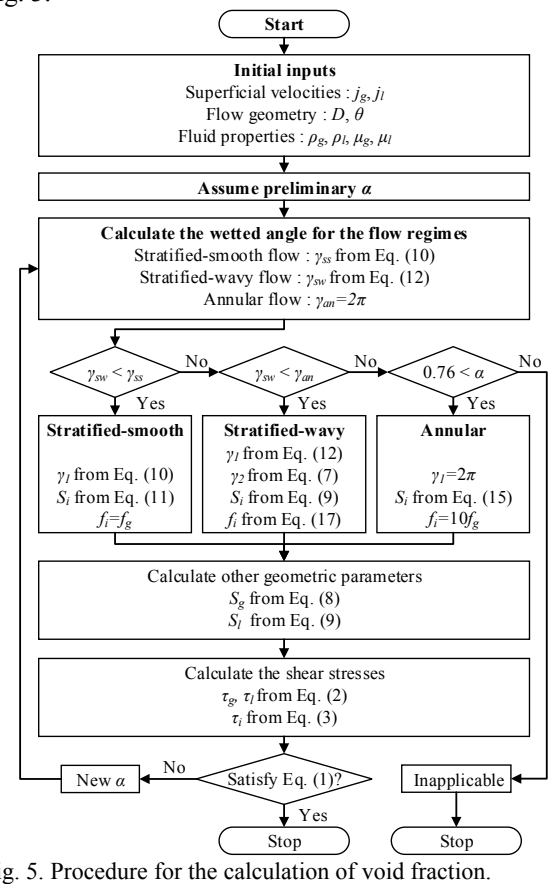

Fig. 5. Procedure for the calculation of void fraction.

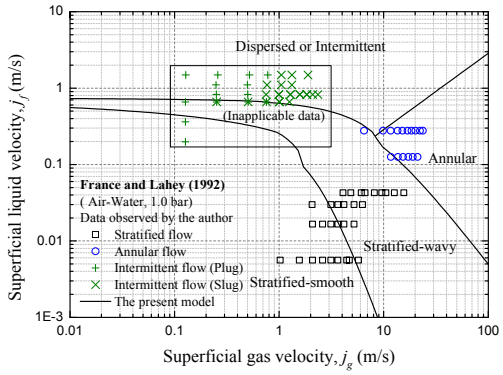

Fig. 6. Comparison of flow regime identification with data by France and Lahey [10].

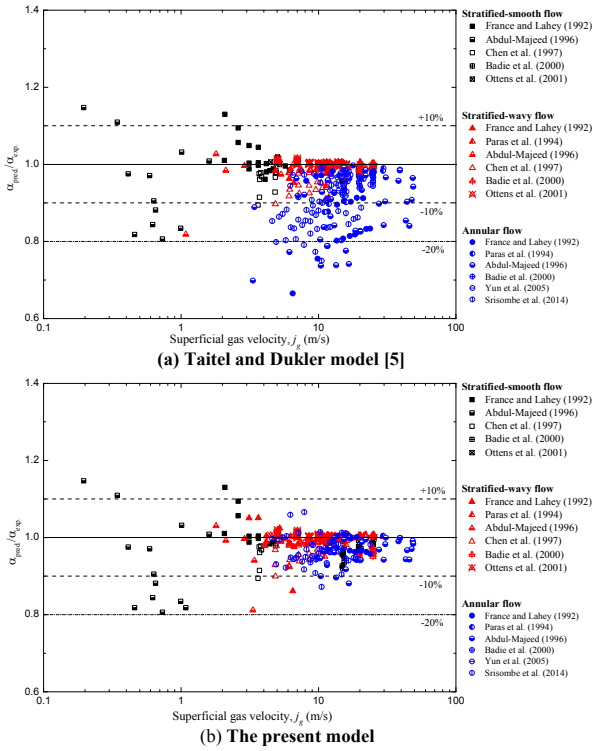

Fig. 7. Comparison of void fraction prediction with available data

4. Conclusions

An improved mechanistic model was proposed to predict accurately the void fraction in the nearly-horizontal tube under the separated flow condition. The model is formulated with a separated flow momentum balance equation so that it is applicable to a broad range of tube sizes, fluid properties and flow conditions. The flow regime transition criteria were determined based on the geometric configuration of an ideal arc-shaped interface. Furthermore, the interfacial friction factor model was also improved by using experimental data so that the model could calculate the void fraction without any discontinuities at flow regime transitions. Finally, an evaluation of the proposed model against available experimental data covering various types of fluids, flow regimes, pipe diameters and channel inclination angles showed a satisfactory agreement.

ACKNOWLEDGMENTS

This work was supported by Nuclear Research & Development Program of the NRF (National Research Foundation of Korea) grant funded by the MSIP(Ministry of Science, ICT and Future Planning) and by the Nuclear Safety Research Center Program of the KORSAFe grant funded by Nuclear Safety and Security Commission (NSSC) of the Korean government (Grant code: NRF-2012M2B2A6028182, 1305011).

NOMENCLATURE

A	cross-sectional area (m^2)
c	constant in the friction factor
D	tube inner diameter (m)
Fr	Froude number
f	friction factor
G	total mass velocity of two phases (kg/m^2-s)
g	gravity acceleration (m/s^2)
j	superficial velocity (m/s)
n	exponent in the friction factor
P	pressure (N/m^2)
R	radius (m)
S	contact perimeter (m)
u	phase velocity (m/s)
x	vapor flow quality
z	coordinate in the downstream direction

Greek symbols

α	void fraction
γ	wetted angle, central angle (rad)
δ	liquid film thickness (m)
θ	Inclination angle, positive for upward flow (°)
μ	dynamic viscosity (N-s/m^2)
ρ	density (kg/m^3)
τ	shear stress (N/m^2)

Subscripts and superscripts

g	gas phase
h	hydraulic equivalent
l	liquid phase
i	interface
w	wall
1	the circle of tube
2	the eccentric circle
*	normalized

REFERENCES

[1] S. Kim, B. U. Bae, Y. J. Cho, Y. S. Park, K. H. Kang, and B. J. Yun, An experimental study on the validation of cooling capability for the Passive Auxiliary Feedwater System (PAFS) condensation heat exchanger, Nuclear Engineering and Design, Vol. 260, p. 54, 2013.
[2] S. S. Jeon, S.J. Hong, J. Y. Park, K. W. Seul, and G. C. Park, Assessment of horizontal in-tube condensation models using MARS code. Part I: Stratified flow condensation, Nuclear Engineering and Design, Vol. 254, p. 254, 2013.
[3] S. S. Jeon, S.J. Hong, J. Y. Park, K. W. Seul, and G. C. Park, Assessment of horizontal in-tube condensation models using MARS code. Part II: Annular flow condensation, Nuclear Engineering and Design, Vol. 262, p. 510 2013.
[4] T. H. Ahn, B. J. Yun, J. J. Jeong, K. H. Kang, Y. S. Park, J. Cheon, and D. W. Jerng, Development of a new condensation model for the nearly-horizontal heat exchanger tube under the steam flowing conditions, International Journal of Heat and Mass Transfer, Vol. 79, p. 876, 2014.
[5] Y. Taitel and A. E. Dukler, A model for predicting flow regime transitions in horizontal and near horizontal gas-liquid flow, AIChE Journal, Vol. 22, no. 1, p. 47, 1976.
[6] T. Fukano and A. Ousaka, Prediction of the circumferential distribution of film thickness in horizontal and near-horizontal gas-liquid annular flows, International Journal of Multiphase Flow, Vol. 15, no. 3, p. 403, 1989.
[7] D. Barnea, Transition from annular flow and from dispersed bubble flow—unified models for the whole range of pipe inclinations, International Journal of Multiphase Flow, Vol. 12, no. 5, p. 733, 1986.
[8] Thome, John R., J. El Hajal, and A. Cavallini. Condensation in horizontal tubes, part 2: new heat transfer model based on flow regimes, International Journal of Heat and Mass Transfer , Vol. 46, no. 18, p. 3365 , 2003.
[9] J. Hart, P. J. Hamersma, and J. M. H. Fortuin, Correlations predicting frictional pressure drop and liquid holdup during horizontal gas-liquid pipe flow with a small liquid holdup, International Journal of Multiphase Flow, Vol. 15, no. 6, p. 947, 1989.
[10] F. França and R. T. Lahey Jr, The use of drift-flux techniques for the analysis of horizontal two-phase flows, International Journal of Multiphase Flow, Vol. 18, no. 6, p. 787, 1992.
[11] S. V. Paras, N. A. Vlachos, and A. J. Karabelas, Liquid layer characteristics in stratified—Atomization flow, International journal of multiphase flow, Vol. 20, no. 5, p. 939, 1994.
[12] G. H. Abdul-Majeed, Liquid holdup in horizontal two-phase gas—liquid flow, Journal of Petroleum Science and Engineering, Vol. 15, no. 2, p. 271, 1996.
[13] X. T. Chen, X. D. Cal, and J. P. Brill, Gas-liquid stratified-wavy flow in horizontal pipelines, Journal of energy resources technology, Vol. 119, no.4, p. 209, 1997.
[14] S. Badie, C. P. Hale, C. J. Lawrence, and G. F. Hewitt, Pressure gradient and holdup in horizontal two-phase gas–liquid flows with low liquid loading, International Journal of Multiphase Flow, Vol. 26, no. 9, p. 1525, 2000,.
[15] M. Ottens, H. C. J. Hoefsloot, and P. J. Hamersma, Correlations predicting liquid hold-up and pressure gradient in steady-state (nearly) horizontal co-current gas-liquid pipe flow, Chemical Engineering Research and Design,Vol, 79, no. 5, p. 581, 2001.
[16] R. Srisomba, O. Mahian, A. S. Dalkilic, and S. Wongwises, Measurement of the void fraction of R-134a flowing through a horizontal tube, International Communications in Heat and Mass Transfer, Vol. 56, p. 8, 2014.
[17] C. J. Crowley, G. B. Wallis, and J. J. Barry, Validation of a one-dimensional wave model for the stratified-to-slug flow regime transition, with consequences for wave growth and slug frequency, International journal of multiphase flow, Vol. 18, no. 2, p. 249, 1992.